Recovery and reuse of Ni(II) from rinsewater of electroplating industries

P. Gomathi Priya [a], C. Ahmed Basha [b,*], V. Ramamurthi [a], S. Nathira Begum [b]

[a] Department of Chemical Engineering, A.C. College of Technology, Anna University, Chennai 600025, India
[b] Central Electro Chemical Research Institute (CSIR), Karaikudi 630006, India

ARTICLE INFO

ABSTRACT

Discharge of nickel compounds, which may occur in both liquid and solid phases, can cause severe environmental problems. In this work, 'point of source' treatment strategy is followed and reduced the nickel content of rinsewater to about less than $1 \, mg \, L^{-1}$ by ion-exchange method using a packed column involving batch recirculation mode of operation and to recovered Ni(II) content by desorption. The treated water could be recycled for rinsing operation.

The nickel from resin is first precipitated as nickel hydroxide to synthesize positive active material and that was used in Nickel/Metal hydride cell. The performances in terms of electrochemical utilization of nickel hydroxide, specific capacity as a function of discharge current density and cycle life were examined and the nickel hydroxide electrode with 5% $CaCO_3$ addition, having $200 \, mAh \, g^{-1}$ specific capacity, could be subjected to charge/discharge cycles at $C/5$ rate for more than 200 cycles without the capacity fading.

© 2008 Elsevier B.V. All rights reserved.

1. Introduction

Many plating and battery industries release heavy metals such as cadmium, lead, chromium and nickel in wastewaters. These heavy metals that find many useful applications in our life are very harmful if discharged into natural water resources and pose a serious health hazard [1–8]. The Ni(II) concentration in wastewater from mine drainage, tableware plating, metal finishing and forging has been reported up to $130 \, mg \, L^{-1}$ [9]. The higher concentration of Ni(II) in ingested water may cause severe damage to lungs, kidneys, gastrointestinal distress, e.g., nausea, vomiting, diarrhea, pulmonary fibrosis, renal edema, and skin dermatitis [3]. It is also a known carcinogen [4]. The rinsewater [10], from Nickel plating industries having nickel concentrations of $2–900 \, mg \, L^{-1}$ is known to be one of the major toxic pollutants, which necessitates the development of effective and inexpensive methods to recover heavy metal and purify rinse water in a closed-recycle system for water reuse (to achieve a so-called effluent-free technology). Conventional methods for the removal of Ni(II) from wastewaters include chemical precipitation, chemical reduction, flocculation, filtration, evaporation, solvent extraction, biosorption, activated carbon adsorption, ion-exchange, reverse osmosis, electrodialysis, membrane separation processes, etc. The chemical precipitation [11], is the most cost-effective treatment technology. The possibility to precipitate metals in the form of insoluble compounds, mostly metal hydroxides, in solutions containing complexing agents depends on the complex stability constant and the hydroxide solubility product. Adsorption by activated carbon is widely used for the removal of toxic metal and has been studied extensively. In addition to conventional activated carbons, some low cost waste materials such as coir pith [12], hazelnut shell [13], almond husk [14], are also utilized for preparation of activated carbon and applied for nickel removal. The removal Ni(II) by clays [15,16], was used in the fabrication of common products like wall or floor tiles, where nickel ions remain firmly attached and inertized. Higher cation-exchange capacity and development of surface negative charge on clay particles in contact with water also contribute to this promising performance, despite the lower available specific surface area in comparison with granular activated carbon. These methods have several disadvantages of high operating cost, incomplete removal, low selectivity, high energy consumption, and they generate hazardous solid waste that are difficult to eliminate.

A broad range of biomass types including bacteria, algae, yeast, fungi, activated sludge, anaerobic sludge, digested sludge, peat have been used as biosorbents to remove Ni(II) metals from aqueous solution [17–40]. The nickel ion, compared with other heavy metal ions, was a more recalcitrant pollutant and many metal tolerant micro-algae had a relatively low Ni-binding capacity. The removal of nickel ions from electroplating effluent was far from satisfactory. The biosorption of nickel by different strains of microorganisms was less than that of other metal ions. This was probably due to the intrinsic chemical properties of nickel ions leading to steric hindrance of biosorption. Studies focusing specifically on nickel removal are rare. There is still no satisfactory precedent of employ-

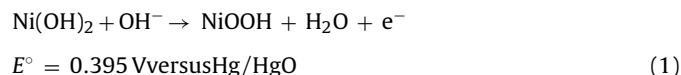* Corresponding author. Tel.: +91 4565 227550; fax: +91 4565 227713.
E-mail addresses: cab_50@yahoo.co.in, basha@cecri.res.in (C.A. Basha).

ing biosorbent in the removal of nickel ions and the feasibility of employing micro-algae to remove Ni from electroplating wastewater is uncertain.

Ion exchange has been widely applied for removal of heavy metal ions from electroplating effluent because it is effective and easy to operate. Recovery and removal of nickel ions from wastewater using ion-exchange method [41–46], was used. However, ion-exchange resins must be regenerated by additive chemical reagents (acid and alkali) when they are saturated and this causes serious secondary pollution. As an alternative technique, electro-dialysis is not economical for treating dilute solution because of its high electrical resistance and the development of concentration polarization phenomena. The combination of electrodialysis and ion-exchange methods (electro-deionization) can be applied to the removal of Ni(II) ions [47–55], from diluted solutions. Electrodeionization includes two processes, which are carried out simultaneously: concentration of ions in the ion exchanger (sorption) and transport of ions through the ion exchanger and membrane system caused by a potential gradient and presence of oxidizing impurities in the solution to be purified results in destruction of the resin. The possibilities of electrochemical technology to remove nickel from dilute industrial solutions were reviewed critically [56]. It is inefficient to first deposit nickel and then dissolve. It may be more efficient to make a concentrated solution of nickel using a hybrid ion-exchange/electrodialysis system. Recently, the development of new technologies as alternatives to traditional methods is required to treat wastewaters, the $Mg(OH)_2$-nanotubes/Al_2O_3 composite membranes [57], oxidized multi-wall carbon nanotubes [58], can be reused to remove Ni^{2+} from water repeatedly with still high effectiveness. The superior performances of metal ions removal are preliminary interpreted and are presumably ascribed decisively to the nanostructures.

The objective this paper is to develop an efficient effluent-free technology to reduce the nickel content of rinse water to about less than $1\,mg\,L^{-1}$ so that the treated water could be recycled for rinsing and subsequently to workout methodology to recover Ni(II) by ion exchange using a packed column involving batch recirculation mode of operation. The recovered Ni(II) from resin could used either for making up the plating bath or alternatively the recovered Ni(II) from the resin could be precipitated as nickel hydroxide to synthesize positive active material that can be used in Nickel/Metal hydride cell.

The active material in the nickel electrode has a theoretical specific capacity $289\,mAh\,g^{-1}$ according to the equation

$$Ni(OH)_2 + OH^- \rightarrow NiOOH + H_2O + e^-$$

$$E° = 0.395\,V\,versus\,Hg/HgO \tag{1}$$

The performances in terms of electrochemical utilization of nickel hydroxide, specific capacity as a function of discharge current density and cycle life were analyzed and reported.

2. Materials and methods

All the reagents and chemicals used were of analytical grade. For adjusting the pH of the medium 0.1N solutions of NaOH and HCl were used. Based on the practical data collected from different plating industries, the synthetic rinsewater of Ni(II) ion of appropriate concentrations were prepared by diluting the nickel electrolytic plating bath of the following composition: $200\,g\,L^{-1}$ of $NiSO_4$, $40\,g\,L^{-1}$ of $NiCl_2$ and $40\,g\,L^{-1}$ of boric acid in water. The solution prepared in this method resembles the rinsewater that found in the actual rinse tank. All the solutions were made with double distilled water. The Amberlite IR-120 cation-exchange resin (density: $0.8\,g\,mL^{-1}$, effective particle size: 0.45–0.6 mm) was used for

all the experiments. Before using them, the resins were soaked in double distilled water for 12 h and then they were rinsed several times also with double distilled water.

2.1. Batch mode adsorption equilibrium studies

The adsorption capability of Amberlite IR-120 cation-exchange resin towards Ni(II) ions was investigated using the synthetic rinsewater. Adsorption experiments were carried out at pH values where no chemical precipitation of $Ni(OH)_2$ occurs. Accordingly the initial pH value of 5.8 for rinsewater was fixed for the adsorption of Ni(II) ions on cation-exchange resin. Adsorption of Ni(II) ions of $440\,mg\,L^{-1}$ was conducted by contacting different weighed amounts of exchange resin (7.8, 4.3, 3.2, 2.6, 2.3, 2, 1.9, 1.8, 1.7, 1.6, 1.5 g) with working volume of 100 mL in 250 mL Erlenmeyer flasks under fixed pre-established conditions. Equilibrium was thoroughly verified for the systems from preliminary experiments performed for different prolonged contact times. The flasks containing the resins were kept in a shaker (with the agitation speed of 160 rpm) at controlled temperature (30 °C) for a period of 12 h. The pH of the slurries was recorded at the start and at the end of each experiment to check for any significant pH drift during the adsorption tests. For the higher resin doses, the marginal drift was noticed in the maintained pH values (within 0.8 units). Once equilibrium was attained, the slurries were filtered and equilibrium concentrations were determined. Nickel analysis was performed using a VARIAN Model SPECTRAA 220, atomic absorption spectrophotometer.

Ni(II) uptake, q_e ($mg\,g^{-1}$ resin), in equilibrium condition was calculated from $q_e = (C_o − C_e)V/W$, where V is the volume sample (in liters), C_o and C_e are the initial and final equilibrium concentrations ($mg\,L^{-1}$) of Ni(II) and W is the amount of resin (in grams).

2.2. Adsorption column breakthrough studies

The experimental arrangement is shown in Fig. 1a and it consists of column of graduated Perspex of 2.25 cm inner diameter and 30 cm height. The Perspex column was equipped with a bottom filtration device to prevent the escape of fine resin beads during processing. In each column test, the ion-exchange resin was first soaked in deionized water for at least 12 h to ensure that the resin was fully swelled prior to use. The column was then loaded with 50 g (15 cm) of the resin. The synthetic rinse water of Ni(II) ion of appropriate concentration was passed downward through the column by a peristaltic pump at a fixed flow rate at the room temperature of (30 °C and initial pH of 5.8). A series of experiments were conducted with various influent concentrations ($160\,mg\,L^{-1}$, $210\,mg\,L^{-1}$ and $440\,mg\,L^{-1}$) and keeping the column height as 15 cm (50 g). The flow rate of the solution was kept at $20\,mL\,min^{-1}$. The samples were collected at certain time intervals and were analyzed for Ni(II) using atomic absorption spectrophotometer (VARIAN Model SPECTRAA 220). The above set experiments were repeated by keeping the flow rate of the solution at $30\,mL\,min^{-1}$. The column data obtained are breakthrough curves for analysis.

2.3. Adsorption column batch recirculation mode studies

One possible mode of operation of IX column is that involves the continuous recirculation of the rinse water. Due to this, there is a gradual depletion of the concentration of Ni(II) ion in the reservoir of rinse water. The operation is shown in Fig. 1a to conduct experiments under batch continuous recirculation mode. The effluent was taken in the reservoir, which was allowed to flow from the reservoir and was recirculated through the packed column using a peristaltic pump and back to the reservoir itself. The experi-
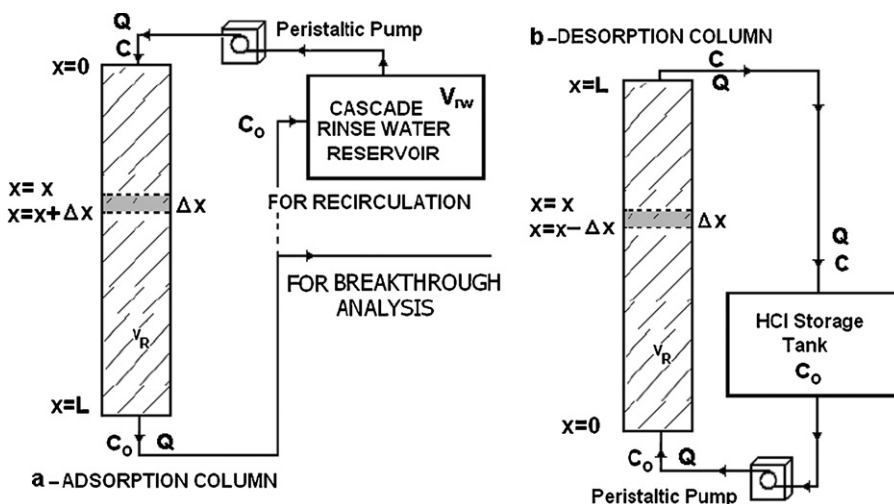
Fig. 1. Experimental setup for IX dynamic column studies: (a) adsorption column for breakthrough analysis and for batch recirculation mode of operations. (b) Desorption column for batch recirculation mode of operations.

ments were conducted at a constant bed height of 15 cm and with an initial concentration of 350 mg L^{-1} for five different flow rates, viz. 10, 15, 20, 25, 30 mL min^{-1}. The samples were drawn periodically from the reservoir and analyzed. The experiments were also repeated at constant flow rate of 30 mL min^{-1} for different concentrations (150, 250, 350, 450, 550 mg L^{-1}). The holdup of the packed reactor is 25 mL where as the reservoir capacity is 3 L. The concentration–time behaviour of the reservoir in a recirculation mode IX system is depicted by normalized concentration versus time plots.

2.4. Column regeneration and reuse studies

Fixed bed ion-exchange column with bed depth of 15 cm and diameter of 2.25 cm was selected for this study for which the adsorption breakthrough curve has been shown. When adsorption process was carried out with initial concentration of 440 mg L^{-1} and flow rate as 30 mL min^{-1}, it was observed that at about 2 h, the column was exhausted. The extra Ni(II) rinse solution inside the column was pumped out leaving only resin loaded with Ni(II) ion. Desorption was carried out slightly at higher temperature 40 °C by 2 mol L^{-1} HCl solution (containing 200 mg L^{-1} Ni(II) ion initially) at a flow rate of 30 mL min^{-1} through the bed in the upward direction to reservoir under recirculation mode. The reservoir volume fixed for this mode of operation was 500 mL. The concentration of Ni(II) in the reservoir was monitored at different time interval. It was observed that desorption cycle took one hour, after which further desorption was negligible.

The performance of IX column was also studied for second adsorption–desorption cycles. The desorbed column was washed with 500 mL distilled water at a flow rate of 35 mL min^{-1} followed by reactivation with 0.01 mg L^{-1} NaOH with a flow rate of 10 mL min^{-1} and finally washing it again with 500 mL distilled water at a flow rate of 35 mL min^{-1}, all in upflow direction of the column. The reactivated and regenerated column was reused for second cycle of adsorption–desorption of Ni(II) keeping the parameters same as above, for first cycle.

2.4.1. Preparation of nickel hydroxide

The chlorides of nickel obtained by desorption processes were precipitated by KOH. The supernatant solution was tested for its minimum concentration of nickel and it was found to be 1 mg L^{-1}. The filtrate was to be recycled through IX column for recovery.

A solution of KOH was added to chlorides of nickel (obtained by desorption) by dripping at a flow rate of 10 mL min^{-1} with constant stirring. The addition of the reagent was terminated when the pH of the suspension reaches 13. Then the mixture was allowed to stand for 24 h for digestion of the precipitate. The separation of the precipitate from the excess reagent was done by centrifugation at 1500 rpm for one hour. The precipitate was washed thoroughly with distilled water. AgNO$_3$ in excess was added to wash water, causing precipitation of silver chloride. The washing of the precipitate was concluded when the white precipitate of silver chloride was no more found in the wash water. This nickel hydroxide precipitate was dried at 90 °C for 72 h. Finally the precipitate was pulverized and sieved. The material with a particle size of the 50 μm was chosen for electrode preparation.

2.4.2. Preparation of Nickel hydroxide electrodes

Because of the poor electric conductivity of the nickel hydroxide powder alone could not be used for electrode fabrication. Certain amount of conductive material, e.g. acetylene black is added to the electrode material. Because of its chain structure, low density and good water absorption characteristics, acetylene black can increase the void and electrode surface per unit volume, and thus improve the contact of the active material with the electrolyte solution. Therefore, increasing the content of acetylene black will improve the utilization. On the other hand, when the Ni(OH)$_2$ content is too high the electrode resistance becomes excessive and thus utilization goes down. So a mere increase in Ni(OH)$_2$ content will not improve the utilization efficiency. If the Ni(OH)$_2$ is increased above the optimum amount, the utilization decreases by virtue of the simultaneous decrease in the void ratio. Conductance decrease with increase in the Ni(OH)$_2$ content, which hinders the electron transfer between Ni(OH)$_2$ particles, i.e. the internal resistance becomes more and thus the capacity decreases [59]. The electrodes are prepared using certain amount of binder, poly tetra fluoro ethylene (PTFE) solution, to bind the particles effectively. Increasing PTFE solution content enhances the utilization. Although it increases the electrode intensity, further increase will decrease the capacity because of the increase in internal resistance. An optimum amount of PTFE solution produces a fibrous structure that holds the active material powder [60]. After considering all the above factors, the following composition of the electrode material was arrived at: 80% Ni(OH)$_2$ powder, 12% nickel powder, 7% acetylene black and 2–5%

PTFE solution. Similar compositions have been suggested by others [61].

The test electrode was made by first mixing the prepared sample nickel hydroxide powder with acetylene black and PTFE solution in the form of slurry. The resulting slurry was packed into a sponge like nickel porous body support (INCO Nickel FOAM) which has a porosity of 95%. The resulting electrode was dried at 65 °C and pressed under 25 mPa to a thickness of 1 mm to have the dimensions: 2 cm × 2 cm × 0.1 cm. Studies were carried out using the following types of electrodes: Nickel hydroxide with no additives and Nickel hydroxide and 5% calcium carbonate incorporated directly in to the slurry.

2.4.3. Test procedure

For all experimental measurements, a three compartment glass cell was used. A hydrogen storage alloy electrode, with a capacity well in excess of the nickel electrode was used as a counter electrode. A single nickel test electrode was sandwiched between two metal hydride electrodes with a thin film of cel-gard separator (Hoechst Celanese Corporation, USA) and the assembly was immersed in 30% aqueous KOH solution. Hg/HgO/KOH electrode was employed as a reference electrode. Constant current charge discharge experiments were performed by using an automatic life cycle tester LCN Bitrode model 2-10-12. The test cell was charged for 14 h at $C/10$ rate and kept for 30 min at open circuit condition and then discharged at the $C/10$ rate to 1.000 V versus a metal hydride electrode [61]. The same procedure was adopted for three cycles until the discharge capacity became constant. Charge/discharge experiments were conducted only after the test cell reached a stable condition.

3. Theoretical description

The monolayer Langmuir and the empirical Freundlich isotherms that can be used to explain the equilibrium adsorption characteristics are the most commonly used models.

3.1. Langmuir isotherm

The Langmuir equation, which is, valid for monolayer sorption on to a surface a finite number of identical sites and is given by Eq. (2).

$$\frac{C_e}{q_e} = \frac{1}{Q^o b} + \frac{C_e}{Q^o} \tag{2}$$

where Q^o is the maximum amount of the Ni(II) ion adsorbed per unit weight of cation-exchange resin to form a complete monolayer (on the surface bound at high C_e), a practical limiting adsorption capacity when the surface is fully covered with Ni(II) ion; and b is a constant related to the affinity of the binding sites. Q^o and b can be determined from the linear plot of C_e/q_e versus C_e.

3.2. Freundlich Isotherm

The empirical Freundlich equation based on sorption on a heterogeneous surface is given below by Eq. (3).

$$q_e = K_F C_e^{1/n} \tag{3}$$

where K_F and n are the Freundlich constants characteristic on the system. K_F and n are indicators of adsorption capacity and adsorption intensity, respectively. According to the Freundlich equation, the amount adsorbed increases infinitely with increasing concentration. This equation is, therefore, satisfactory for low concentrations. The Freundlich isotherm is also more widely used

but provides no information on the monolayer adsorption capacity, in contrast to the Langmuir model.

The adsorption capacity parameter obtained from a batch experiment is useful in providing information about the effectiveness of Ni(II) ion-resin exchange system. However, the data obtained under batch conditions are generally not applicable to most treatment systems (such as column operations). Hence, there is a need to perform dynamic studies as breakthrough analysis using columns. The general position of the breakthrough curve along the volume axis depends on the capacity of the column with respect to the feed concentration and flow rate. The breakthrough curve would be a step function for favorable separations, i.e. there would be an instantaneous jump in the effluent concentration from zero to the feed concentration at the moment the column capacity is reached. The breakthrough curves show the loading behaviour of Ni(II) to be removed from solution in a fixed bed and is usually expressed in terms of adsorbed Ni(II) concentration or normalized concentration defined as the ratio of effluent Ni(II) concentration to inlet Ni(II) concentration (C/C_o) as a function of time or volume of effluent for a given bed height.

Concentration and flow rate on Ni(II) ion adsorption by ion-exchange column were investigated. Thomas model and Adams–Bohart model were used to predict the performance.

3.3. Thomas model

The expression of Thomas model for an adsorption column is given as follows [62,63]:

$$\frac{C}{C_o} = \frac{1}{1 + \exp((k_{Th}/Q)(q_o X - C_o V_{eff}))} \tag{4}$$

where k_{Th} is the Thomas rate constant (mL min^{-1} mg^{-1}); q_o is the equilibrium Ni(II) uptake per g of the adsorbent (mg g^{-1}). X is the amount of adsorbent in the column (g); V_{eff} is effluent volume (mL); C_o is the influent Ni(II) concentration (mg L^{-1}); C is the effluent concentration (mg L^{-1}) at time t; Q is flow rate (mL min^{-1}). The value of t is time (min, $t = V_{eff}/Q$). The kinetic coefficient k_{Th} and the adsorption capacity of the column q_o can be determined from a plot of $\ln(C_o/C - 1)$ against t at a given flow rate using the linear regression method.

3.4. The Adams–Bohart model

The Adams–Bohart model is used for the description of the initial part of the breakthrough curve. The expression is the following [62,63]:

$$\frac{C}{C_o} = \exp\left(k_{AB} C_o t - k_{AB} N_0 \frac{Z}{U_o}\right) \tag{5}$$

where k_{AB} is the kinetic constant (L mg^{-1} min^{-1}), U_o is the superficial velocity calculated by dividing the flow rate by the column section area (cm min^{-1}), Z is the bed depth of column and N_0 is the saturation concentration (mg L^{-1}). From this equation, values describing the characteristic operational parameters of the column can be determined from a plot of $\ln C/C_o$ against t at a given bed height and flow rate using the linear regression method.

3.5. Column with Batch recirculation system

In order to design the plant for IX processes, development of the models is essential which explains variation of concentration of Ni(II) ion with time in the reservoir which is assumed to be perfectly back-mix system. Plug flow exists in IX column. Hence the concentration of Ni(II) changes in the column axially. The transport of

the reactive ions in the exchange column occurs under convective-diffusion control which is a good approximation. The particle size, d_p of ion-exchange resin does not change during the process. The mass transfer coefficient k_p is constant throughout the bed. Rinse-water temperature and hence physical properties is constant both in space and time. Referring to Fig. 1a which also depicts an element of reactor length Δx and in this problem the concentration C is a function of both position x and time t, a differential mass balance at plane x gives the following partial differential equation

$$-A \, \Delta x \frac{\partial C}{\partial t} = Q \left(\frac{\partial C}{\partial x} \right) \Delta x + A \, \Delta x \frac{6(1-\varepsilon)}{d_p} k_p C \quad (6)$$

Left hand side (LHS) represents rate of change of mass of Ni(II) in the pore volume of the ion-exchange column, where v_R is the void volume of the column, ε is the bed porosity. The first term of the right hand side (RHS) rate of mass of Ni(II) ion entering and leaving the differential element where Q is the volumetric flow rate. The next term represents the rate of disappearance of mass of nickel ions in the solution due to sorption of nickel ions in resins phase. As a matter of fact for dilute solutions, sorption of nickel ion in resins is usually diffusion-controlled and, it is generally admitted that external transfer is the rate-controlling process [64]. The driving force being the concentration difference through the diffusion film and the expression should be $[6(1-\varepsilon)/d_p]k_p(C-C^*)$ here k_p is the mass transfer coefficient to the particle surface d_p the particle diameter, and C^* the concentration at the interface particle–film. Owing to the high exchange capacity of the resin, to the weak concentration in solution and to the relatively long duration of the experiments, the amount of nickel ion on the resin is always little significant. Thus, the concentration near the resin surface remains zero during the experiments. Assuming phase equilibrium, the concentration in the solution near the interface, C^* is zero, which leads to $[6(1-\varepsilon)/d_p]k_p C$.

The reservoir (rinse water tank) is always a perfectly back-mix system. Hence the mass balance equation for the rinse water reservoir tank is,

$$V_{rw} \left(\frac{dC}{dt} \right) = QC_o - QC \quad (7)$$

where V_{rw} is the volume of the rinse water reservoir tank.

Since there is no accumulation of the nickel ion in liquid phase IX bed, it can also be assumed that the reactor is under steady state condition as $dC/dt = 0$. The concentration variation of Ni(II) ion in the ion-exchange compartment is written as

$$-\left(\frac{dC}{dx} \right) = \left(\frac{6(1-\varepsilon)A}{Q} \right) \frac{k_p}{d_p} C \quad (8)$$

$$\frac{C_o}{C} = \exp \left(-\frac{[6(1-\varepsilon)/d_p]v_R k_p}{Q} \right) = \exp(-k_p a \tau_R) \quad (9)$$

where a is specific surface area $[6(1-\varepsilon)/d_p]$ of ion-exchange resin, and τ_R is the residence time of nickel ion (v_R/Q) in the ion-exchange column. The mass balance Eq. (7) is solved after substitution of the expression for C_o from Eq. (9), knowing the initial concentration of nickel ion, $C = C^o$ at $t = 0$ in reservoir. Then the following resultant
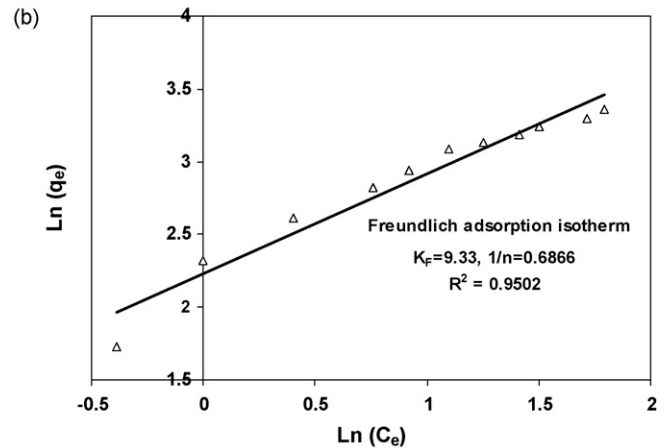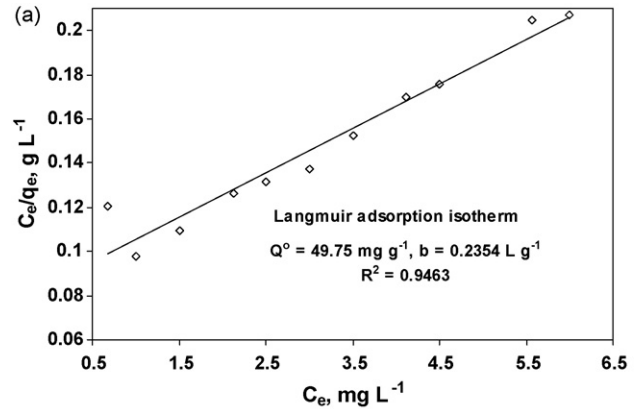

Fig. 2. Isotherm plots for adsorption of Ni(II) ion to resin $C_o = 440$ mg L^{-1}, $W = [7.8, 4.3, 3.2, 2.6, 2.3, 2, 1.9, 1.8, 1.7, 1.6, 1.5 \text{ g}]$, batch volume = 0.1 L. (a) Langmuir and (b) Freundlich.

equation gives the variation of concentration of Ni(II) in the effluent reservoir.

$$\frac{C}{C^o} = \exp \left[-\frac{t}{\tau} \left\{ 1 - \exp(-k_p a \tau_R) \right\} \right] \quad (10)$$

where C^o is the initial concentration of nickel and τ is the residence time of nickel ion (V_{rw}/Q) in the effluent reservoir, respectively.

It is to be noted that C/C^o decreases exponentially with time. In accordance with Eq. (10), the slope of the plot of $\ln(C/C^o)$ versus t is $[1 - \exp(-k_p a \tau_R)]/\tau$ from which the value of $k_p a$, the transfer coefficient is computed.

When the reservoir of regeneration tank (see Fig. 1b) is considered, which is also a perfectly back-mix system, the mass balance equation for the regeneration reservoir tank is,

$$V_{rg} \left(\frac{dC_o}{dt} \right) = QC_o - QC \quad (11)$$

where V_{rg} is the volume of the regeneration reservoir tank.

Table 1
Thomas and Adams–Bohart model parameters at different conditions of influent concentration and flow rate using linear regression analysis

C_o (mg L^{-1})	Q (mL min^{-1})	k_{Th} (L mg^{-1} min)	q_o (mg L^{-1})	R^2	k_{AB} (L mg^{-1} min)	N_o (mg L^{-1})	R^2
160	20	0.169	21505.7	0.99531	0.00015	18562.6	0.99688
160	30	0.231	16978.6	0.97482	0.0002	22037.2	0.98357
210	20	0.195	20316.1	0.99286	0.00017	17877.3	0.99429
210	30	0.277	23986.1	0.99836	0.00025	20341.9	0.997
440	20	0.216	23726.9	0.97785	0.00023	18970.5	0.99919
440	30	0.346	25192.9	1	0.00032	20953.3	0.99887

Since there is no accumulation of the nickel ion in liquid phase of ion-exchange desorption column, it can be assumed that the reactor to be under steady state condition as $dC/dt = 0$. The concentration variation of Ni(II) ion in the ion-exchange column is written as

$$\left(\frac{dC}{dx}\right) = \left(\frac{6(1-\varepsilon)A}{Q}\right)\frac{k_p}{d_p}C \tag{12}$$

$$\frac{C}{C_o} = \exp\left(\frac{[6(1-\varepsilon)/d_p]v_R k_p}{Q}\right) = \exp(k_p a \tau_R) \tag{13}$$

where a is specific surface area $[6(1-\varepsilon)/d_p]$ of ion-exchange resin, and τ_R is the residence time of nickel ion (v_R/Q) in the ion-exchange column. The mass balance Eq. (9) is solved after substitution of the expression for C_o from Eq. (10), knowing the initial concentration of nickel ion, $C = C^o$ at $t = 0$ in reservoir. Then the following resultant equation gives the variation of concentration of Ni(II) in the regeneration reservoir.

$$\frac{C}{C^o} = \exp\left[\frac{t}{\tau_{rg}}\left\{\exp(k_p a \tau_R) - 1\right\}\right] \tag{14}$$

where C^o is the initial concentration of nickel and τ_{rg} is the residence time of nickel ion (V_{rg}/Q) in the regeneration reservoir, respectively.

3.6. Error analysis

The least sum of the squares, SS, of the differences between the experimental data and the data obtained from the models (by calculation), could be computed. If data from the model are similar to the experimental data, SS will be a small number; if they are different, SS will be a large number. In order to confirm the best fit isotherm for the column adsorption system, it is necessary to analyze the data using the values of SS, combined with the values of the determined coefficient (R^2).

4. Results and discussion

The results of the experiments carried out are presented in Figs. 1–8 and Tables 1–3.

4.1. Ni(II) equilibrium adsorption isotherms

Linear plots (Fig. 2a and b) of C_e/q_e versus C_e and $\ln(q_e)$ versus $\ln C_e$ show that the adsorption obeys both Langmuir and Freundlich isotherm models. The high values of coefficient of regression (R^2) for both the models indicate good agreement between experimental and predicted data. The applicability of both the isotherm
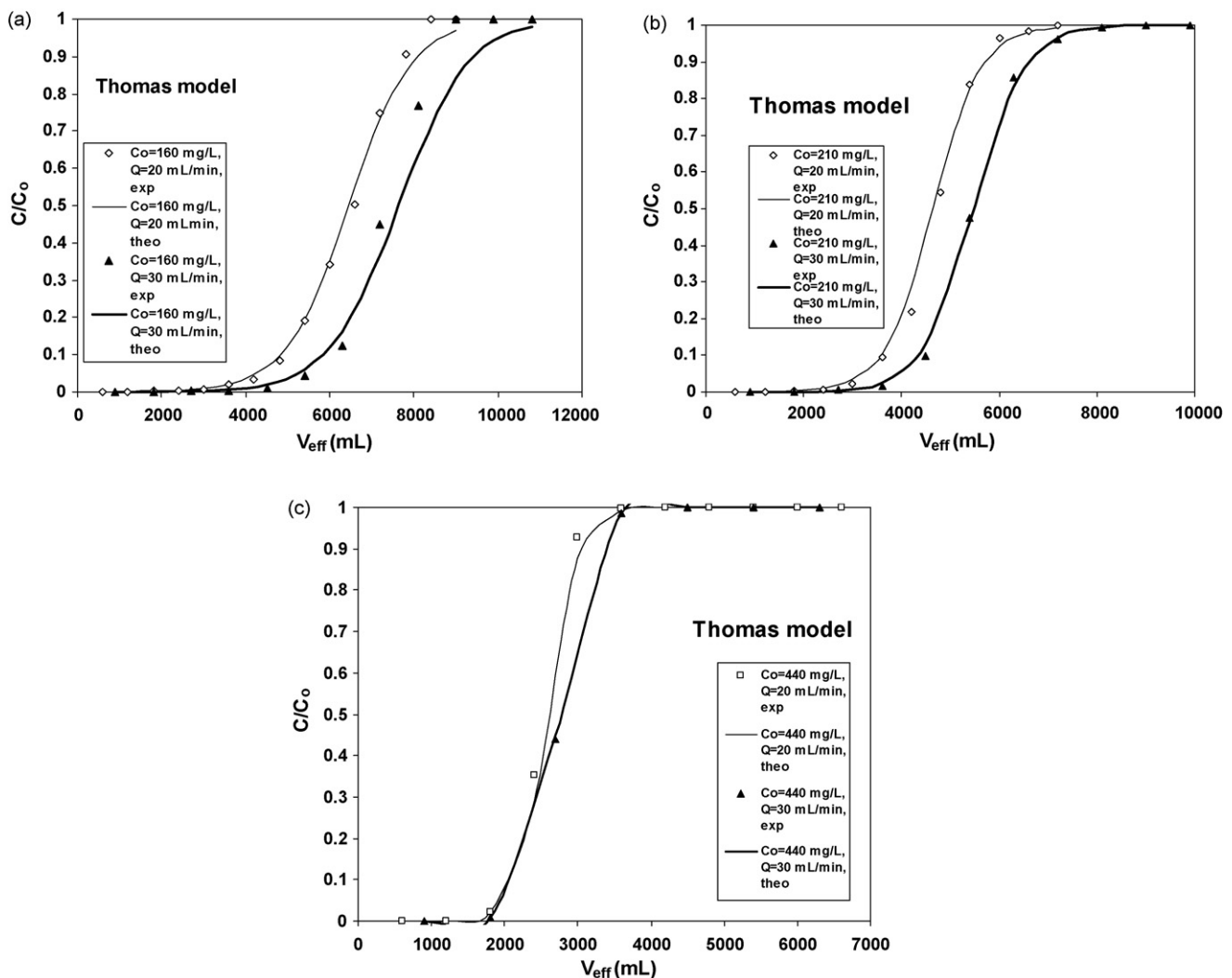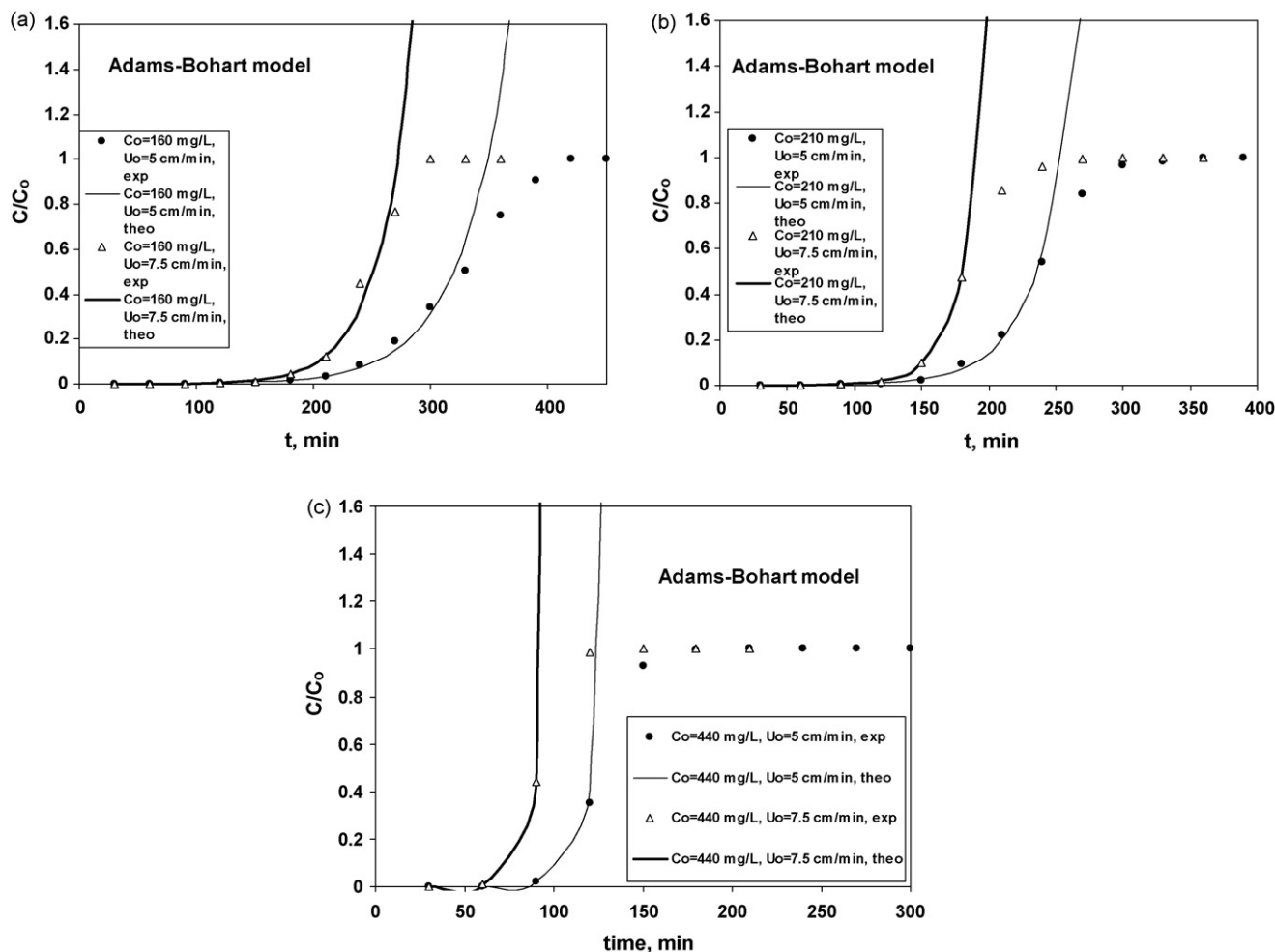

Fig. 3. The experimental and predicted breakthrough curves at different flow rates and feed concentration at constant bed height of 0.15 m according to the Thomas model: (a) 160 mg L^{-1}, (b) 210 mg L^{-1} and (c) 440 mg L^{-1}.

Fig. 4. The experimental and predicted breakthrough curves at different flow rates and feed concentration at constant bed height of 0.15 m according to the Adams–Bohart model: (a) 160 mg L^{-1}, (b) 210 mg L^{-1} and (c) 440 mg L^{-1}.

Table 2
Effect of mass transfer coefficient of packed ion-exchange adsorption column at constant bed height: (a) $C_o = 350$ mg L^{-1} and different flow rates and (b) $Q = 30$ mL/min and different initial concentration

Q (mL min^{-1})	$C_o = 350$ mg L^{-1}		C_o (mg L^{-1})	$Q = 30$ mL min^{-1}	
	$k_p a$ ($\times 10^{-2}$ s^{-1})	k_p ($\times 10^{-4}$ cm s^{-1})		$k_p a$ ($\times 10^{-2}$ s^{-1})	k_p ($\times 10^{-4}$ cm s^{-1})
10	1.4419	2.07	150	2.8834	4.14
15	1.0788	1.55	250	1.8501	2.66
20	1.0796	1.55	350	1.4685	2.11
25	1.4941	2.15	450	1.0388	1.49
30	1.4679	2.11	550	0.7963	1.14

models to the Ni(II)-cation-exchange resin system implies that both monolayer sorption and heterogeneous surface conditions exit under the experimental conditions used. The sorption of Ni(II) ions on the resin is thus complex, involving more than one mechanism.

In case of Langmuir model, maximum adsorption capacity, Q^0 (mg g^{-1}), was found to be 49.75 mg of Ni(II) per g of resin where as the affinity constant, b (L g^{-1}) is 0.2354 L g^{-1}. The essential characteristics of Langmuir isotherm model can be explained in term of a dimensionless constant separation factor or equilibrium parameter R_L, which is defined by $R_L = 1/(1 + bC_o)$ and the R_L value is between 0 and 1 indicate favorable adsorption of Ni onto resin.

Table 3
Specific discharge capacity of active materials with and without CaCO$_3$

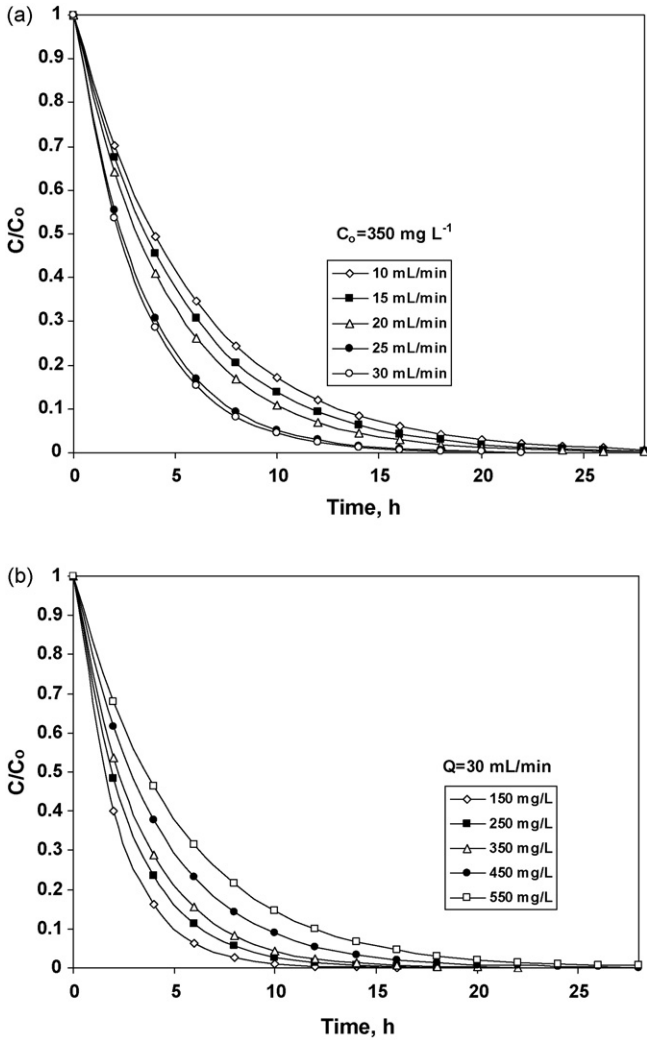| Discharge rate	Specific capacity (mAh g^{-1})	
	With no additives	With additives CaCO$_3$
$C/10$	210	225
$C/5$	190	230
1 C	150	215

Fig. 5. Concentration–time behaviour of the reservoir in a recirculating ion-exchange adsorption column at constant bed height: (a) $C_o = 350 \, mg \, L^{-1}$ and different flow rates and (b) $Q = 30 \, mL/min$ and different initial concentration.

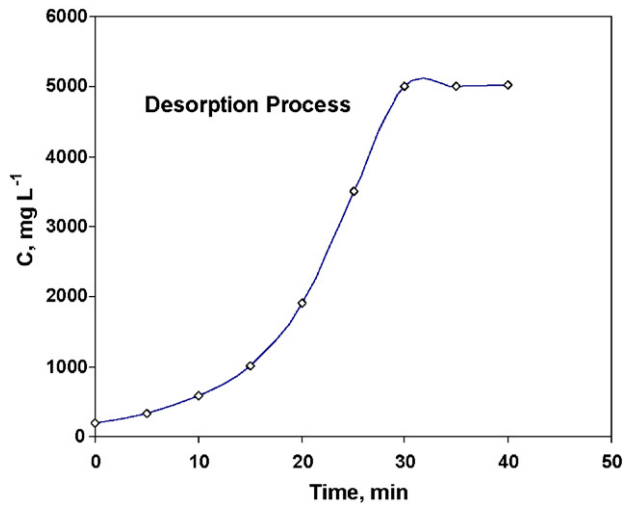**Fig. 6.** Concentration–time behaviour of the reservoir in a recirculating ion-exchange desorption column at constant bed height: $C_o = 200 \, mg \, L^{-1}$ and $Q = 30 \, mL/min$.
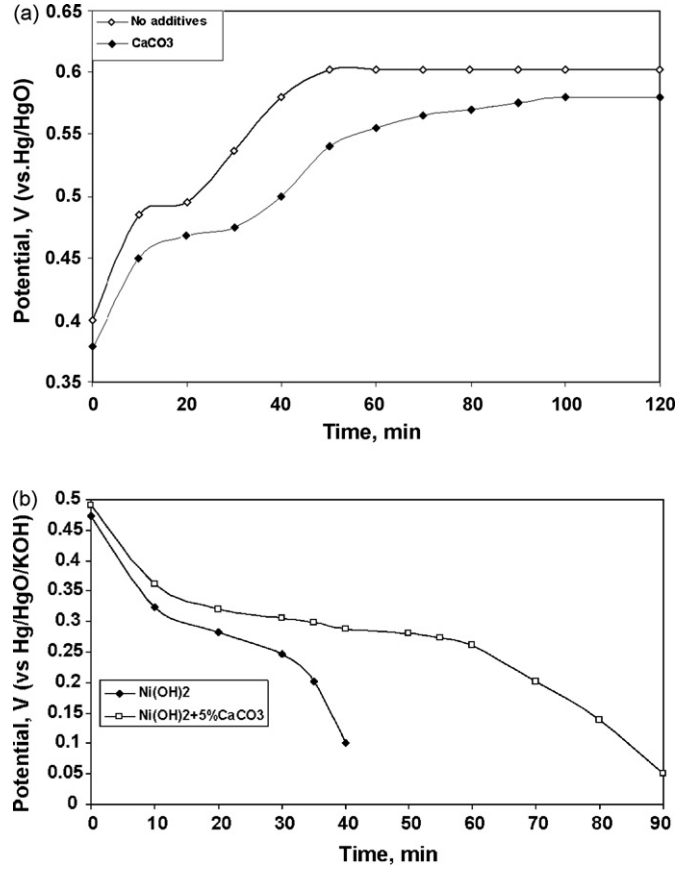

Fig. 7. The characteristics of nickel electrodes with and without addition of $CaCO_3$ (a) at $C/5$ rate charging and (b) at $C/5$ rate discharging.

The constants of Freundlich isotherm K_F and n which relate to sorption capacity and sorption intensity are 9.33 and 1.4565, respectively. According to Treyball [65], it has been shown using mathematical calculations that n values between 1 and 10 represents beneficial adsorption.

4.2. Adsorption column breakthrough analysis

Successful design of a column adsorption process requires prediction of the concentration–time profile or breakthrough curve for the effluent. The time for breakthrough appearance and the shape of the breakthrough curve are very important characteristics for determining the operation and the dynamic response of an adsorption column.
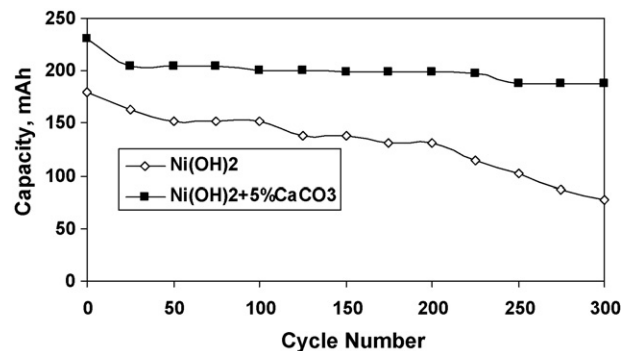

Fig. 8. The cycle life performance of the two types of electrodes under study at $C/5$ rate.

The experimental and the predicted breakthrough curves at different flow rates and feed concentrations at constant bed height of 15 cm are shown according to the Thomas model in Fig. 3a–c; and to the Adams–Bohart model in Fig. 4a–c.

The column data were fitted to the Thomas model to determine the Thomas rate constant (k_{Th}) and maximum solid-phase concentration (q_o). The determined coefficients and relative constants were obtained using linear regression analysis ($\ln(C_o/C - 1)$ against t), a modified form of Eq. (4) and the results are listed in Table 1. From Table 1, it is seen that values of determined coefficients (R^2) is higher than 0.97. Hence it is clear from Fig. 3 and Table 1 there was a good agreement between the experimental and predicted normalized concentration values at experimental conditions. So the data obtained fits Eq. (4) well.

It is to be observed from Table 1 that as the influent concentration increased the value of q_o and k_{Th} increased. The reason is that the driving force for sorption is the concentration difference between the Ni(II) ion on the resin and the Ni(II) ion in the solution. Thus the high driving force due to the higher Ni(II) ion concentration resulted in better column performance. The bed capacity q_o and k_{Th} increased with the flow rate increasing at the influent Ni(II) ion concentration of 440 mg L^{-1} and 210 mg L^{-1} and on other hand at the influent at 160 mg L^{-1} the bed capacity q_o decreased while k_{Th} increased with the flow rate increasing. The Thomas model is suitable for adsorption processes when the external and internal diffusions will not be the limiting step.

The Adams–Bohart adsorption model was applied to experimental data for the description of the initial part of the breakthrough curve. This approach was focused on the estimation of characteristic parameters, such as maximum adsorption capacity (N_o) and kinetic constant (k_{AB}) from Adams–Bohart model. After applying Eq. (5) to the experimental data, the parameters were obtained for the relative concentration region upto 50% breakthrough. Using linear regression analysis for all breakthrough curves, respective values of N_o, and k_{AB} were calculated and presented in Table 1 (together with the regression coefficients, R^2). From Table 1 it is seen that the values of N_o at all conditions have no significant difference. It is clear from Fig. 4 and Table 1 that there is a good agreement between the experimental and predicted values, suggesting that the Adams–Bohart model will be valid for the relative concentration region up to 0.5 where large discrepancies can be found between the experimental and predicted curves above this level for the Ni(II) ion adsorption column. The Adams–Bohart model provides a simple and comprehensive approach to running and evaluating sorption-column tests and valid to the range of conditions used.

4.3. Batch recirculation mode operation

To develop an efficient effluent-free technology to reduce the nickel content of rinse water to about less than 1 mg L^{-1} so that the treated water could be recycled for rinsing and subsequently to workout methodology to recover Ni(II) by ion exchange using a packed column involving batch recirculation mode of operation and the results of experiments are shown in Fig. 6a and b.

The slope of the plot of $\ln(C/C^o)$ versus t is $[1 - \exp(-k_p a\tau_R)]/\tau$ which was obtained from Eq. (10) by linear regression. The value of $k_p a$, k_p, the mass transfer coefficient is computed and presented in Table 2. The goodness of fit is more than 0.98, which is the evidence for the model to fit well.

From Table 2, as the influent concentration increased, the value of mass transfer coefficient k is decreased slightly. The driving force for sorption is the concentration difference between the Ni(II) ion on the resin and the Ni(II) ion in the solution diminishes on recirculation but due to the higher Ni(II) ion concentration resulted in

better column performance in a single pass because of high driving force on the other hand the mass transfer coefficient k changes insignificantly with increase of flow rate at the influent concentration of 350 mg L^{-1}.

The transfer coefficient $k_p a$ can be estimated using the available dimensional relationship [66], between the dimensionless numbers.

$$k_p a = \frac{10.9 U (1 - \varepsilon)}{d_p} \left(\frac{UD}{d_p} \right)^{0.51} \left(\frac{D\rho}{\mu} \right)^{0.16} \quad (15)$$

where U is the superficial velocity (volumetric flow rate of fluid per unit area of the bed cross section), D is the fluid-phase diffusivity, ρ is density; and μ is viscosity, in consistent units. With the above relationship, the obtained value of $k_p a$ is 0.14464 for the flow rate 10 mL/min while the experimental value is 0.014419. The calculated value is around 10 times higher than the experimental value. The difference probably indicates that the treatment process functions not via the whole bed but through a smaller length of it, an "absorption front". Initially, this front concerns the initial input region, and with time this region is inactive and the adsorption front proceeds toward the output region.

4.4. Column regeneration, recovery and reuse

The loaded metal from the column is desorbed in the smallest possible volume of in the reservoir in the batch recirculation mode. Regeneration must produce small volume of metal concentrates suitable for metal-recovery process, without damaging the capacity of the resin, making it reusable in several adsorptions and desorption cycles. The result of desorption process carried out by 2 mol L^{-1} HCl solution (containing 200 mg L^{-1} Ni(II) ion initially) at a flow rate of 30 mL min^{-1} through the bed in the upward direction to reservoir under recirculation mode is shown in Fig. 6. The reservoir volume fixed for this mode of operation was 500 mL. The performance of the reactivated and regenerated column (with 0.01 mol/l NaOH and distilled water) was highly efficient in adsorption and desorption. Regeneration of the adsorbent material is of crucial importance in the development of effluent-free technology as desorbed metal concentrates can be added to plating bath for making up the plating bath or alternatively the recovered Ni(II) from the resin could be precipitated as nickel hydroxide to synthesize positive active material to be used in Nickel/Metal hydride cell. The result of the experiments conducted shown in Table 3. The specific capacities of electrodes with no additive and with calcium carbonate prepared under same conditions are listed.

The specific capacity of the active materials with calcium compound is higher than that of the active material without additive, particularly at higher discharge rates. From Table 3 it is found that the capacities of the nickel electrode containing calcium increase gradually with discharge rate and the decrease is very slowly at higher rate.

The charge/discharge characteristics of nickel electrodes, without addition and with CaCO$_3$ at $C/5$ rate are shown in Fig. 7a and b. The redox reaction of the nickel electrode is expressed as given in Eq. (1). But here it should be noted that the oxygen evolution occurs at an electrode potential above +0.400 V versus Hg/HgO which is slightly above the open circuit potential of nickel hydroxide electrodes. Thus the oxygen evolution cannot be avoided during charging process according to the reaction

$$4OH^- \rightarrow 2H_2O + O_2 + 4e^- \quad (16)$$

For an electrode with no additive, the oxygen evolution reaction takes place easily and this will lower the charging efficiency. With addition of calcium compound, however, the oxygen evolu-

tion overpotential increased markedly (Fig. 7a). This effect hinders the oxygen evolution reaction and increases greatly the charging efficiency and thus more utilization of active materials.

The structure of nickel hydroxide is dependent not only on the history of the electrode material but also on additives like calcium compounds. Fig. 7b shows the discharge characteristics of nickel electrodes with and without additives. Fig. 8 shows the cycle life performance of the two types of electrodes the charge efficiency and the discharge efficiency is increased. Calcium has been found to raise the oxygen evolution over potential hence effects increase the charge acceptance and the discharge depth of the nickel electrodes.

5. Conclusions

Adsorption of Ni(II) ion from simulated rinsewater on Amberlite IR-120 cation-exchange resin followed both Langmuir and Freundlich adsorption isotherm models. The Thomas and the Adams–Bohart models were applied to experimental data obtained from dynamic studies performed on fixed column to predict the breakthrough curves and to determine the column kinetic parameters. The initial region of breakthrough curve was defined by the Adams–Bohart model at all flow rates and inlet Ni(II) ion concentrations studied while the full description of breakthrough could be accomplished by the Thomas models at higher flow rates and higher inlet Ni(II) ion concentrations. The model constants belonging to each model were determined by linear regression technique and these parameters could be uses for in column design over a range of feasible flow rates and concentrations.

In the packed IX column involving batch recirculation mode of operation, there is a gradual depletion of Ni(II) ion concentration in reservoir and when its concentration attains less than $1\,mg\,L^{-1}$ then the treated water could be recycled for rinsing so as to conserve water. The adsorbed Ni(II) ion was effectively desorbed with the use of mineral acid with high the regeneration efficiency under batch recirculation mode of operation. The recovered Ni(II) from resin is used for making up the plating bath so that the total process is made sustainable. Alternatively the recovered Ni(II) from the resin could be precipitated as nickel hydroxide to synthesize positive active material to be used in Nickel/Metal hydride cell so as to make a value added byproduct. The experimental results showed that incorporation of calcium compound into the electrode invoked excellent charge–discharge behaviour.

Based on the above concept further work is under progress with two packed IX columns in series involving batch recirculation mode of operation with the cascade of reservoirs rinse tank. When the first column exhausted it will be replaced by the second column and the second column will be replaced by a new one. The exhausted column is taken for regeneration.

References

[1] E. Denkhaus, K. Salnikow, Nickel essentially, toxicity, and carcinogenicity, Oncology/Hematology 42 (2002) 35–56.
[2] E.F. Pane, J.G. Richards, C.M. Wood, Acute waterborne nickel toxicity in the rainbow trout (*Oncorhynchus mykiss*) occurs by a respiratory rather than iono-regulatory mechanism, Aquat. Toxicol. 63 (2003) 65–82.
[3] N.R. Axtell, S.P.K. Sternberg, K. Claussen, Lead and nickel removal using microspora and lemna minor, Bioresour. Technol. 89 (2003) 41–48.
[4] N. Akhtar, J. Iqbal, M. Iqbal, Removal and recovery of nickel(II) from aqueous solution by loofa sponge-immobilized biomass of *Chlorella sorokiniana*: characterization studies, J. Hazard. Mater. B108 (2004) 85–94.
[5] E.F. Pane, A. Haque, C.M. Wood, Mechanistic analysis of acute, Ni-induced respiratory toxicity in the rainbow trout (*Oncorhynchus mykiss*): an exclusively branchial phenomenon, Aquat. Toxicol. 69 (2004) 11–24.
[6] E.F. Pane, C. Bucking, M. Patel, C.M. Wood, Renal function in the freshwater rainbow trout (*Oncorhynchus mykiss*) following acute and prolonged exposure to waterborne nickel, Aquat. Toxicol. 72 (2005) 119–133.
[7] E.F. Pane, M.D. McDonald, H.N. Curry, J. Blanchard, C.M. Wood, M. Grosell, Hydromineral balance in the marine gulf toadfish (*Opsanus beta*) exposed to waterborne or infused nickel, Aquat. Toxicol. 80 (2006) 70–81.
[8] Eric F. Pane, Monika Patel, Chris M. Wood, Chronic, sublethal nickel acclimation alters the diffusive properties of renal brush border membrane vesicles (BBMVs) prepared from the freshwater rainbow trout, Comp. Biochem. Physiol., Part C 143 (2006) 78–85.
[9] S. Erdogan, Y. Onal, C. Akmil-Basar, S. Bilmez-Erdemoglu, C. Sarici-Ozdemir, E. Koseoglu, G. Icduygu, Optimization of nickel adsorption from aqueous solution by using activated carbon prepared from waste apricot by chemical activation, Appl. Surf. Sci. 252 (5) (2005) 1324–2133.
[10] J.W. Patterson, Industrial Wastewater Treatment Technology, 2nd ed., Butterworth Publisher, Stoneham, MA, 1985.
[11] O. Gyliene, J. Aikaite, O. Nivinskiene, Recycling of Ni(II)–citrate complexes using precipitation in alkaline solutions, J. Hazard. Mater. B109 (2004) 105–111.
[12] K. Kadirvelu, K. Thamaraiselvi, C. Namasivayam, Adsorption of nickel(II) from aqueous solution onto activated carbon prepared from coirpith, Sep. Purif. Technol. 24 (3) (2001) 497–505.
[13] E. Demirbas, M. Kobya, S. Oncel, S. Sencan, Removal of Ni(II) from aqueous solution by adsorption onto hazelnut shell activated carbon: equilibrium studies, Bioresour. Technol. 84 (3) (2002) 291–293.
[14] H. Hasar, Adsorption of nickel(II) from aqueous solution onto activated carbon prepared from almond husk, J. Hazard. Mater. 97 (1–3) (2003) 49–57.
[15] G.E. Marquez, M.J.P. Ribeiro, J.M. Ventura, J.A. Labrincha, Removal of nickel from aqueous solutions by clay-based beds, Ceram. Int. 30 (2004) 111–119.
[16] S.S. Gupta, K.G. Bhattacharyya, Adsorption of Ni(II) on clays, J. Colloid Interface Sci. 295 (2006) 21–32.
[17] M.E. Argun, S. Dursun, K. Gur, C. Ozdemir, M. Karatas, S. Dogan, Nickel adsorption on the modified pine tree materials, Environ. Technol. 26 (2005) 479–488.
[18] S.S. Shukla, L.J. Yu, K.L. Dorris, A. Shukla, Removal of nickel from aqueous solutions by sawdust, J. Hazard. Mater. 121 (2005) 243–246.
[19] S. Pradhan, S.S. Shukla, K.L. Dorris, Removal of nickel from aqueous solutions using crab shells, J. Hazard. Mater. 125 (2005) 201–204.
[20] K. Vijayaraghavan, J. Jegan, K. Palanivelu, M. Velan, Removal of nickel(II) ions from aqueous solution using crab shell particles in a packed bed up-flow column, J. Hazard. Mater. 113 (2004) 223–230.
[21] E. Malkoc, Y. Nuhoglu, Investigations of nickel(II) removal from aqueous solutions using tea factory waste, J. Hazard. Mater. 127 (1–3) (2005) 120–128.
[22] E. Malkoc, Y. Nuhoglu, Removal of Ni(II) ions from aqueous solutions using waste of tea factory: adsorption on a fixed-bed column, J. Hazard. Mater. 135 (2006) 328–336.
[23] I. Villaescusa, N. Fiol, M. Martinez, N. Miralles, J. Poch, J. Serarols, Removal of copper and nickel ions from aqueous solutions by grape stalks wastes, Water Res. 38 (4) (2004) 992–1002.
[24] F. Abu Al-Rub, M. Kandah, N. Aldabaibeh, Nickel removal from aqueous solutions using sheep manure wastes, Eng. Life Sci. 2 (4) (2002) 111–116.
[25] Y.S. Ho, D.A. John Wase, C.F. Forster, Batch nickel removal from aqueous solution by *Sphagnum* moss peat, Water Res. 29 (5) (1995) 1327–1332.
[26] A. Selatinia, A. Madni, M.Z. Bakhti, L. Kertous, Y. Mansouri, R. Yous, Biosorption of Ni²⁺ from aqueous solution by NaOH-treated bacterial dead *Streptomyces rimosus* biomass, Min. Eng. 17 (2004) 903–911.
[27] F.A. Abu Al-Rub, M.H. El-Nass, F. Benyahia, I. Ashour, Biosorption of nickel on blank alginate beads, free and immobilized algal cells, Process Biochem. 39 (2004) 1767–1773.
[28] S. Kalyani, P. Srinivasa Rao, A. Krishnaiah, Removal of nickel(II) from aqueous solutions using marine macroalgae as the sorbing biomass, Chemosphere 57 (2004) 1225–1229.
[29] C.E. Borba, R. Guirardello, E.A. Silva, M.T. Veit, C.R.G. Tavares, Removal of nickel(II) ions from aqueous solution by biosorption in a fixed bed column: experimental and theoretical breakthrough curves, Biochem. Eng. J. 30 (2006) 184–191.
[30] H. Xu, Y. Liu, J.-H. Tay, Effect of pH on nickel biosorption by aerobic granular sludge, Bioresour. Technol. 97 (2006) 359–363.
[31] M. Yalvac Can, Y. Kaya, O.F. Algur, Response surface optimization of the removal of nickel from aqueous solution by cone biomass of *Pinus sylvestris*, Bioresour. Technol. 97 (2006) 1761–1765.
[32] E. Malkoc, Ni(II) removal from aqueous solutions using cone biomass of *Thuja orientalis*, J. Hazard. Mater. 137 (2006) 899–908.
[33] P.K. Wong, K.Y. Fung, Removal and recovery of nickel ion (Ni²⁺) from aqueous solution by magnetite-immobilized cells of Enterobacter sp. 4–2, Enzyme Microb. Technol. 20 (1997) 116–121.
[34] Y.S. Ho, G. McKay, Pseudo second order model for sorption processes, Process Biochem. 34 (1999) 451–465.
[35] J.P.K. Wong, Y.S. Wong, N.F.Y. Tam, Nickel biosorption by two chlorella species, *C. vulgaris* (a commercial species) and *C. miniata* (a local isolate), Bioresour. Technol. 73 (2000) 133–137.
[36] Q. Yu, P. Kaewsarn, Adsorption of Ni2+ from aqueous solutions by pretreated biomass of marine macroalga *Durvillaea potatorum*, Sep. Sci. Technol. 35 (5) (2000) 689–701.

[37] A. Lopez, N. Lazaro, S. Morales, A.M. Marques, Nickel biosorption by free and immobilized cells of *Pseudomonas fluorescens* 4F39: a comparative study, Water Air Soil Pollut. 135 (2002) 157–172.

[38] Z. Aksu, Determination of the equilibrium, kinetic and thermodynamic parameters of the batch adsorption of nickel(II) ions onto *Chlorella vulgaris*, Process Biochem. 38 (2002) 89–99.

[39] F.B. Dilek, A. Erbay, U. Yetis, Ni(II) biosorption by *Polyporous versicolor*, Process Biochem. 37 (2002) 723–726.

[40] V. Patmavathy, P. Vasudevan, S.C. Dhingra, Adsorption of nickel(II) ions on Baker's yeast, Process Biochem. 38 (10) (2003) 1389–1395.

[41] A.H. Elshazly, A.H. Konsowa, Removal of nickel ions from wastewater using a cation-exchange resin in a batch-stirred tank reactor, Desalination 158 (1–3) (2003) 189–193.

[42] I. Rodriguez-Iznaga, A. Gomez, G. Rodriguez-Fuentes, A. Benitez Aguilar, J. Serrano-Ballan, Natural clinoptilolite as an exchanger of Ni^{2+} and $2NH_4^+$ ions under hydrothermal conditions and high ammonia concentration, Microporous Mesoporous Mater. 53 (2002) 71–80.

[43] I. Rodriguez-Iznaga, G. Rodriguez-Fuentes, A. Benitez Aguilar, The role of carbonate ions in the ion-exchange $Ni^{2+} = 2NH_4^+$ in natural clinoptilolite, Microporous Mesoporous Mater. 41 (2000) 129–136.

[44] M. Seggiani, S. Vitolo, S. D'Antone, Recovery of nickel from Orimulsion fly ash by iminodiacetic acid chelating resin, Hydrometallurgy 81 (2006) 9–14.

[45] H. Tokuyama, S. Maeda, K. Takahashi, Development of a novel moving bed with liquid-pulse and experimental analysis of nickel removal from acidic solution, Sep. Purif. Technol. 38 (2004) 139–147.

[46] A. Papadopoulos, D. Fatta, K. Parperis, A. Mentzis, K.-J. Haralambous, M. Loizidou, Nickel uptake from a wastewater stream produced in a metal finishing industry by combination of ion-exchange and precipitation methods, Sep. Purif. Technol. 39 (2004) 181–188.

[47] Y.S. Dzyazko, V.N. Belyakov, Purification of a diluted nickel solution containing nickel by a process combining ion exchange and electrodialysis, Desalination 162 (1–3) (2004) 179–189.

[48] P.B. Spoor, W.R. ter Veen, L.J.J. Janssen, Electrodeionization 1: migration of nickel ions absorbed in a rigid, macroporous cation-exchange resin, J. Appl. Electrochem. 31 (2001) 523–530.

[49] P.B. Spoor, W.R. ter Veen, L.J.J. Janssen, Electrodeionization 2: the migration of nickel ions absorbed in a flexible ion-exchange resin, J. Appl. Electrochem. 31 (2001) 1071–1077.

[50] P.B. Spoor, L. Koene, W.R. ter Veen, L.J.J. Janssen, Electrodeionisation 3: the removal of nickel ions from dilute solutions, J. Appl. Electrochem. 32 (2002) 1–10.

[51] P.B. Spoor, L. Koene, L.J.J. Janssen, Potential and concentration gradients in a hybrid ion-exchange/electrodialysis cell, J. Appl. Electrochem. 32 (2002) 369–377.

[52] P.B. Spoor, L. Grabovska, L. Koene, L.J.J. Janssen, W.R. ter Veen, Pilot scale ÿeionization of a galvanic nickel solution using a hybrid ion-exchange/electrodialysis system, Chem. Eng. J. 89 (1–3) (2002) 193–202.

[53] P.B. Spoor, L. Koene, W.R. ter Veen, L.J.J. Janssen, Continuous deionization of a dilute nickel solution, Chem. Eng. J. 85 (2–3) (2002) 127–135.

[54] L.M. Rozhdestvenska, Y.S. Dzyazko, V.N. Belyakov, Electrodeionization of a Ni^{2+} solution using highly hydrated zirconium hydrophosphate, Desalination 198 (2006) 247–255.

[55] Y.S. Dzyazko, Purification of a diluted solution containing nickel using electrodeionization, Desalination 198 (2006) 47–55.

[56] L. Koene, L.J.J. Janssen, Removal of nickel from industrial process liquids, Electrochim. Acta 47 (5) (2001) 695–703.

[57] S. Zhang, F. Cheng, Z. Tao, F. Gao, J. Chen, Removal of nickel ions from wastewater by $Mg(OH)_2/MgO$ nanostructures embedded in Al_2O_3 membranes, J. Alloys Compd. 426 (2006) 281–285.

[58] C. Chen, X. Wang, Adsorption of Ni(II) from aqueous solution using oxidized multiwall carbon nanotubes, Ind. Eng. Chem. 45 (2006) 9144–9149.

[59] D. Yunchang, Y. Jionliang, L. Hui, C. Zhaorong, W. Zeyun, A study of the performance of a paste-type nickel cathode, J. Power Sources 56 (1995) 201–204.

[60] Z. Chang, Y. Zhao, Y. Ding, Effects of different methods of cobalt addition on the performance of nickel electrodes, J. Power Sources 77 (1999) 69–73.

[61] K. Manimaran, S. Nathira Begum, N.G. Ranganathan, M. Rhagavan, Performance and electrochemical characterization of nickel-hydroxide electrodes in nickel metal hydride battery, Trans. SAEST 39 (2004) 44–45.

[62] Z. Aksu, F. Gönen, Biosorption of phenol by immobilized activated sludge in a continuous packed bed: prediction of breakthrough curves, Process Biochem. 39 (2004) 599–613.

[63] R. Han, D. Ding, Y. Xu, W. Zou, Y. Wang, Y. Li, L. Zou, Use of rice husk for the adsorption of congo red from aqueous solution in column mode, Bioresour. Technol. 99 (2008) 2938–2946.

[64] I. Monzie, L. Muhr, F. Lapicque, G. Greǐvillot, Mass transfer investigations in electrodeionization processes using the microcolumn technique, Chem. Eng. Sci. 60 (2005) 1389–1398.

[65] R.E. Trybal, Mass Tranfers Operations, 3rd ed., McGraw, New York, 1980.

[66] R.H. Perry, C.H. Chilton, Chemical Engineers' Handbook, 5th ed., McGraw-Hill, Kogakusha, 1984, pp. 16–20.